Use of an open photoacoustic cell for the thermal characterisation of liquid crystals

N.A. George[1,*], **C.P.G. Vallabhan**[1], **V.P.N. Nampoori**[1], **A.K. George**[2], **P. Radhakrishnan**[1]

[1] International School of Photonics, Cochin University of Science and Technology, Cochin 682 022, India
[2] Physics Department, College of Science, Sultan Qaboos University, P.O. Box 36, Postal Code 123, Muscat, Oman

Abstract. In this paper, we describe the use of an open cell photoacoustic configuration for the evaluation of the thermal effusivity of liquid crystals. The feasibility, precision and reliability of the method are initially established by measuring the thermal effusivities of water and glycerol, for which the effusivity values are known accurately. In order to demonstrate the use of the present method in the thermal characterization of liquid crystals, we have measured the thermal effusivity values in various mesophases of 4-cyano-4′-octyloxybiphenyl (8OCB) and 4-cyano-4′-heptyloxybiphenyl (7OCB) liquid crystals using a variable temperature open photoacoustic cell. A comparison of the measured values for the two liquid crystals shows that the thermal effusivities of 7OCB in the nematic and isotropic phases are slightly less than those of 8OCB in the corresponding phases.

PACS: 81.70.Cv; 43.90.+v; 44.90.+c

Extensive theoretical and experimental studies on the thermal parameters and the critical behaviour of the thermal transport properties of liquid crystals in the vicinity of phase transitions have been reported in the literature [1–3]. However, thermal transport properties, such as thermal diffusivity or effusivity of liquid crystals far away from the phase transition temperatures, still remain a subject for detailed investigations because of their importance in device fabrication. Among the various methods, the ac calorimetric method is one of the most commonly used techniques for the thermal characterisation of liquid crystals [4, 5]. Recently, photoacoustic and photopyroelectric techniques have been successfully implemented, allowing a complete quantitative evaluation of the static and dynamic thermal parameters as well as the study of the critical behaviour of these parameters in liquid crystals [6–8]. The thermal effusivity, e_s, defined by $(k\varrho C)^{1/2}$, which has the dimensions $W\,s^{1/2}\,cm^{-2}\,K^{-1}$, where k the thermal conductivity, ϱ the density and C the specific heat capacity, is a rather abstract thermal quantity. Though the thermal effusivity is a relevant thermophysical parameter for surface heating

or cooling processes, as well as for quenching processes, a direct measurement of this quantity using conventional heat flow methods is not easy. The thermal effusivity measures essentially the thermal impedance of the sample, effectively the sample's ability to exchange heat with the environment. Hence, its value is very significant in the case of liquids and in liquid crystals, especially when these are used as temperature sensors or in temperature sensitive devices.

The aim of this paper is to demonstrate the use of an open cell photoacoustic configuration to accurately measure the thermal effusivity of liquid crystals or any other non-absorbing liquids. To the best of our knowledge this is the first report on the measurement of the thermal effusivities of 4-cyano-4′-octyloxybiphenyl (8OCB) and 4-cyano-4′-heptyloxybiphenyl (7OCB) liquid crystals in various phases other than the crystalline phase. Liquid crystals of this family are well known for their high chemical stability.

1 Theory

The open photoacoustic cell (OPC) is actually a minimum volume photoacoustic configuration, and its details are described elsewhere [9]. Almost all the OPC studies reported to date have been carried out at room temperature. Very recently, N.A. George et al. have demonstrated the use of a variable temperature OPC for the thermal characterization of comb-shaped polymers [10]. Consider an open cell photoacoustic configuration such as that shown in Fig. 1. Let a thermally thin, solid absorbing layer be in contact with a non-absorbing liquid. If this system is exposed to modulated optical radia-
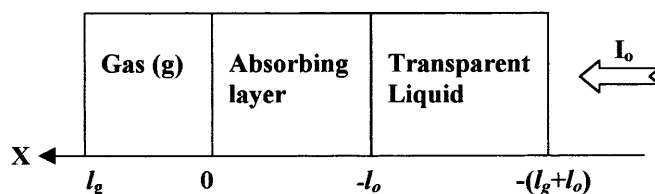

Fig. 1. Geometry of the OPC configuration

*Corresponding author. (E-mail: nibu@cusat.ac.in)

tion, the absorbing layer absorbs the light and heat is generated periodically at the surface of this layer, which is in contact with the liquid sample. The heat generated is diffused through the absorbing layer behind it. The thermal diffusion equations for such a configuration are [11]:

$$\frac{\partial^2 T_s}{\partial x^2} = \sigma_s^2 \, T_s \tag{1a}$$

$$\frac{\partial^2 T_0}{\partial x^2} = \sigma_0^2 \, T_0 - \frac{\beta I_0}{k_0}\delta\,(x + l_0) \tag{1b}$$

and

$$\frac{\partial^2 T_g}{\partial x^2} = \sigma_g^2 \, T_g \tag{1c}$$

where $\sigma_i = (1 + j)a_i$, with $a_i = \left(\frac{\pi f}{\alpha_i}\right)^{\frac{1}{2}}$ and the thermal diffusivity is given by $\alpha_i = \frac{k_i}{\varrho_i C_i}$. Here the suffix i denotes the liquid sample ($i = s$), the absorbing layer ($i = 0$) and the air in the microphone chamber ($i = g$). Assuming that the entire light is absorbed at $x = -l_0$ and solving (1a)–(1c) together with the boundary conditions of temperature and heat flux continuity, one can arrive at the expression for the acoustic pressure in the microphone chamber:

$$\delta Q = \frac{\gamma P_0 \beta I_0}{T_0 l_g \sigma_g k_0 \sigma_0}\left(\frac{\mathrm{e}^{j\omega t}}{b\cosh(l_0\sigma_0) + \sinh(l_0\sigma_0)}\right) \tag{2}$$

where $b = \left(\frac{k_s\sigma_s}{k_0\sigma_0}\right)$, γ is the ratio of heat capacities of air, P_0 and T_0 are the pressure and temperature of the gas inside the chamber, I_0 is the incident radiation intensity, l_g is the length of the gas column in the cavity, β and l_0 are the optical absorption coefficient and thickness of the absorbing layer. Here $\omega = 2\pi f$, where f is the modulation frequency.

For a thermally thin absorbing layer we can assume that $l_0\sigma_0 \ll 1$, in which case the above expression reduces to the form:

$$\delta Q_1 = \frac{\gamma P_0 \beta I_0 \left(\alpha_g \alpha_s\right)^{\frac{1}{2}}}{2\pi T_0 l_g k_s}\frac{\mathrm{e}^{j(\omega t - \pi/2)}}{f} \tag{3}$$

Equation (3) implies that the acoustic signal now varies as f^{-1} and is proportional to the ratio $\frac{\sqrt{\alpha_s}}{k_s} = e_s^{-1}$, the inverse of the thermal effusivity of the transparent liquid.

However, if there is no liquid sample in contact with the absorbing layer, then the pressure fluctuation δQ_2 inside the cavity is given by:

$$\delta Q_2 = \frac{\gamma P_0 \beta I_0 \alpha_g^{\frac{1}{2}}\alpha_0}{(2\pi)^{\frac{3}{2}}T_0 l_g l_0 k_0}\frac{\mathrm{e}^{j(\omega t - 3\pi/4)}}{f^{\frac{3}{2}}} \tag{4}$$

Thus, according to (4), the signal varies as $f^{-\frac{3}{2}}$ and depends on the ratio α_0/k_0. Using this as a reference signal and from the ratio of (3) and (4), one can easily eliminate all the constants and other geometrical parameters determined by the cell. The thermal effusivity of the liquid sample can then be evaluated by measuring the signal amplitude as a function of modulation frequency from the absorbing layer–non-absorbing liquid composite sample and that from the absorbing layer alone, provided the thickness, density and specific heat capacity of the thin layer are known.

2 Experimental

The experimental set-up used for the measurement of the thermal effusivity consisted of an Argon Ion laser (Liconix 5000), an open photoacoustic cell (OPC), a temperature controller, a mechanical chopper and a lock-in amplifier. Modulated optical radiation at 488 nm with a power level of 200 mW was used for the measurements. Both the liquid crystals 7OCB and 8OCB are optically non-absorbers at this wavelength. Investigations were carried out using a variable temperature, resonant, open photoacoustic cell. However, the measurements were carried out far below the resonance frequency (440 Hz) of the cell. A cross-sectional view of the sample-holder and resonant cell is shown in Fig. 2. The liquid crystal sample holder was made of a nylon ring of thickness 3 mm, the bottom of which was closed by a 60-μm-thick copper foil. The copper foil was illuminated at the surface in contact with the liquid sample and the photoacoustic signal was detected at the other side. The microphone compartment and the sample chamber of the PA cell were acoustically coupled through a narrow-bore stainless steel tube of inner diameter 1 mm. Half of the sample holder was filled with the liquid crystal and the sample chamber was heated using a heater coil wound around the chamber The sample temperature was controlled to an accuracy of $\pm0.13\,^\circ$C using a chromel–alumel thermocouple sensor along with a temperature controller. This reasonably good temperature stability was found to give an almost stable photoacoustic signal. The photoacoustic signal was detected using an electret microphone (Knowles BT 1834) and was processed using a lock-in amplifier (Stanford Research Systems SR 510). The signal amplitude was recorded as a function of laser beam modulation frequency for the empty sample holder and after filling it with the liquid crystal sample.
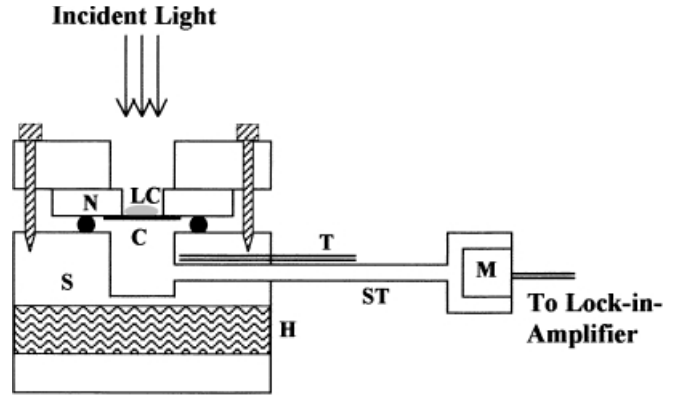

Fig. 2. Cross-sectional view of the open photoacoustic cell. N is the nylon ring, C is the copper foil, LC is the liquid crystal sample, T is the is thermocouple, S is the stainless steel body, H is the heater coil, ST is the stainless steel tube and M is the microphone

3 Results and discussion

Initially, the present experimental approach was verified using water and glycerol as the non-absorbing liquids. These liquids are very transparent in the visible region and their thermal properties are well known. The acoustic signal produced by the empty sample holder and that obtained after

filling it with these liquids was measured as a function of the modulation frequency. The typical variation in the signal amplitude for the glycerol–copper system and the water-copper system at room temperature is shown in Figs. 3 and 4. It is worthwhile to note here that, in either case, the amplitude of the signal produced by the empty sample holder (copper foil alone) was greater than that from the copper–liquid (water or glycerol) composite sample. This indicates that the liquid acts as a heat sink, or a part of the thermal energy generated at the liquid–copper interface is absorbed by the liquid due to its finite thermal conductivity. A comparison of Figs. 3 and 4 also confirms this. The thermal conductivity values of water, glycerol and air are $0.591\,\mathrm{W\,m^{-1}\,K^{-1}}$, $0.270\,\mathrm{W\,m^{-1}\,K^{-1}}$ and $0.0241\,\mathrm{W\,m^{-1}\,K^{-1}}$, respectively [12]. Consequently, water, being a liquid with higher thermal conductivity than glycerol, produced a smaller signal compared to the latter and both the liquids caused a reduction in the signal amplitude compared to that obtained when there was no liquid in the sample holder. Figure 5 shows the $\log(f^{\frac{1}{2}})$ versus $\log(R)$ plot for water and glycerol. Here f is the chopping frequency and $R = (PA_{\mathrm{f}}/PA_{\mathrm{e}})$ where PA_{f} is the signal produced by the liquid filled sample holder and PA_{e} is that from the empty sam-
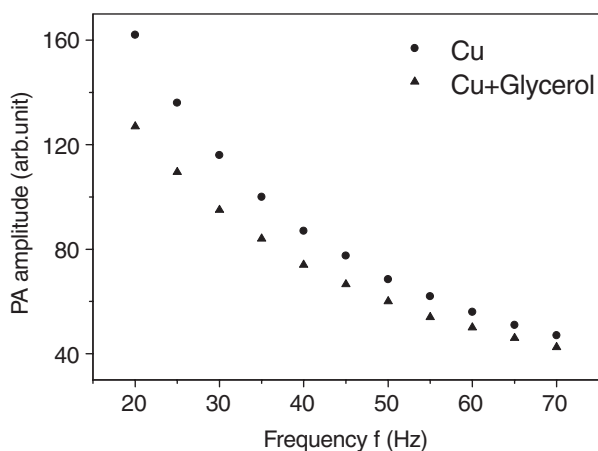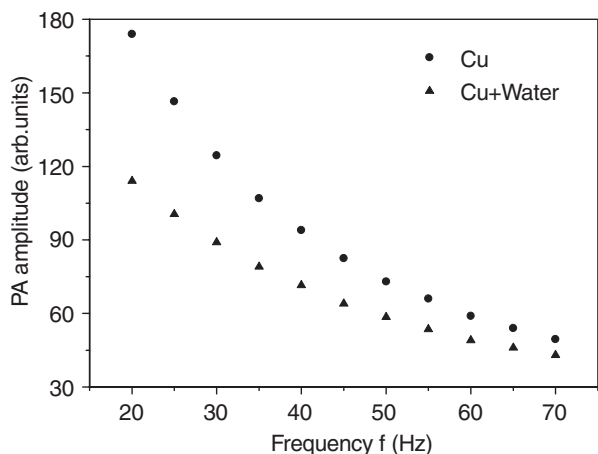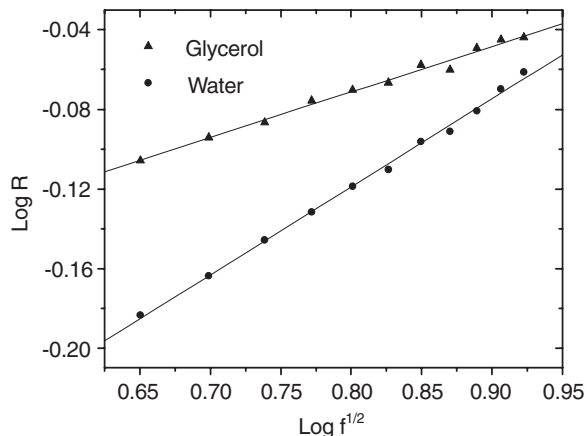
Fig. 5. Logarithmic plot connecting the square root of modulation frequency and the normalized PA signal amplitudes for water and glycerol

ple holder. From a straight line fit to the ratio of the two signal amplitudes, the thermal effusivities were calculated using (3) and (4). The calculated values of the thermal effusivities of water and glycerol were $0.154(\pm0.002)\,\mathrm{W\,s^{1/2}\,cm^{-2}\,K^{-1}}$ and $0.093(\pm0.001)\,\mathrm{W\,s^{1/2}\,cm^{-2}\,K^{-1}}$. The measured values were found to agree well with the literature values of $0.158\,\mathrm{W\,s^{1/2}\,cm^{-2}\,K^{-1}}$ and $0.093\,\mathrm{W\,s^{1/2}\,cm^{-2}\,K^{-1}}$, respectively, for the former and the latter [12]. The density, specific heat capacity and thickness of the copper foil were $\varrho_0 = 8.96\,\mathrm{g\,cm^{-3}}$, $C_0 = 0.385\,\mathrm{J\,g^{-1}\,K^{-1}}$ and $l_0 = 60\,\mu\mathrm{m}$, respectively.
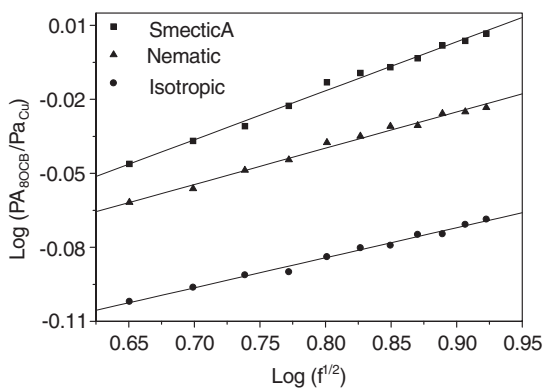
The liquid crystals 8OCB and 7OCB were obtained from Merck Inc, UK and were used without further recrystallization. The literature values for the phase transition temperatures of 8OCB are $54\,°\mathrm{C}$, $67.5\,°\mathrm{C}$ and $80.5\,°\mathrm{C}$, corresponding to the crystalline to smectic A, smectic A to nematic and nematic to isotropic transitions, respectively, and those of 7OCB are $55\,°\mathrm{C}$ and $73.5\,°\mathrm{C}$ for the crystalline to nematic and nematic to isotropic transitions, respectively [13, 14]. We have measured the thermal effusivities of all these phases except the crystalline phase. Measurements were carried out at $60\,°\mathrm{C}$, $72\,°\mathrm{C}$ and $90\,°\mathrm{C}$, respectively, for the 8OCB samples in the smectic A, nematic and isotropic phases. In the case of 7OCB samples, the investigations were performed at $60\,°\mathrm{C}$ and $90\,°\mathrm{C}$, corresponding to the nematic and isotropic phases, respectively. The fixed temperatures for the measurements in each phase were selected so as to ensure that the samples were well stabilized in each phase and were in thermal equilibrium. Even though these liquid crystals are optically non-absorbing at 488 nm, scattering loss in each phase is an important factor to be taken into account. The same sample holder was used to measure the transmitted intensity at 488 nm. For this purpose, the copper foil was replaced by a glass plate (1.5 mm thick), and the surface facing the photoacoustic chamber cavity was coated with carbon black. For an empty sample holder, a linear dependence of the photoacoustic signal amplitude with the incident light intensity was observed. The sample holder was then filled with the liquid crystal and the photoacoustic signal at a constant incident light intensity was recorded. The magnitude of the signal enabled the accurate estimation of the percentage transmittance in each mesophase of the sample. For the same sample thickness as that used for the thermal effusivity measurements

Fig. 3. PA signal variation with modulation frequency for the Cu foil–glycerol composite sample

Fig. 4. PA signal variation with modulation frequency for the Cu foil–water composite sample

(1.5 mm), the optical transmittance (at 488 nm) of 8 OCB at 60 °C, 72 °C and 90 °C was 67%, 71% and 97.4%, respectively. The optical transmittance of 7OCB at 488 nm was measured as 65% and 95.8% at 60 °C and 90 °C, respectively.

A logarithmic plot connecting the square root of the modulation frequency and the ratio of signal amplitudes in each phase of 8OCB with the reference signal is shown in Fig. 6. The estimated values of the thermal effusivities are summarised in Table 1. From the tabulated values of the thermal effusivities, it can be seen that the smectic A phase possesses the minimum thermal effusivity, followed by a slight increase in the nematic phase. The isotropic phase at 90 °C showed the maximum thermal effusivity. The literature values for the heat capacity of 8OCB show a slight increase in the isotropic phase [3, 5]. Also, the variation in the density between the different mesophases is reported to be negligibly small. In terms of the liquid crystal molecular orientation, the nematic phase has the translational symmetry of a fluid, but a broken rotational symmetry characterised by long-range orientational order produced by the alignment of their long molecular axes along the director. In the nematic phase, however, the centres of mass of the molecules are still randomly distributed. Therefore, in the absence of any external magnetic or electric fields to align the molecules in a preferred direction, any measured value of thermal conductivity will be its average value, given by

$$\langle k \rangle = \frac{1}{3} \left(k_x + 2k_y \right) , \tag{5}$$

where k_x and k_y are the thermal conductivities parallel and perpendicular, respectively, to the director in the oriented samples [15]. Since neither density nor specific heat capacity of the liquid crystals are affected by the molecular alignment, we can rewrite the above expression in terms of the thermal effusivity e_s as:
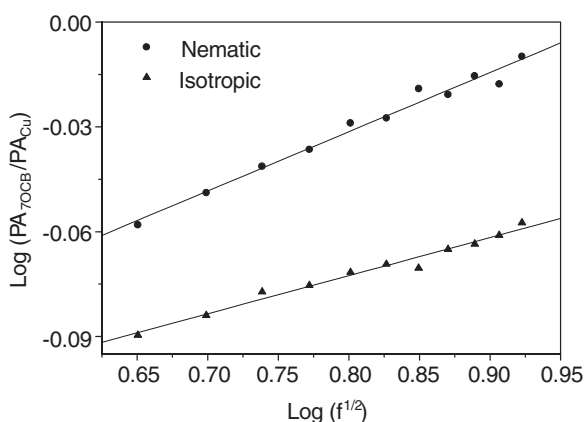
$$\langle e_s \rangle = \frac{1}{3} \left[(e_s)_x + (2e_s)_y \right] . \tag{6}$$

The experimental plot connecting the square root of the frequency and the ratio of signal amplitudes in the logarithmic scale for 7OCB sample is shown in Fig. 7. The thermal effusivity values in the nematic and isotropic phases are summarised in Table 1. In this case also, the thermal effusivity in the nematic phase is lower than that in the isotropic phase. Again, in the nematic phase, the measured value for the thermal effusivity will be the average value contributed by the average thermal conductivity given by (6).

A comparison of the present data with any of the reported thermal parameters of 8OCB or 7OCB is rather difficult because the required parameters at the temperatures we have used are not clearly reported in the literature. Also, heat capacity data varies significantly from sample to sample depending on small changes in their purity [4]. In the present case, the main reason for the decrease in the thermal effusivity value in the nematic phase may be due to the fact that the photoacoustic signal amplitude is mainly determined by a very thin surface layer, called the first thermal diffusion length within the sample. The thermal diffusion length is defined as $\mu = (2\alpha/\omega)^{\frac{1}{2}}$. The thermal diffusion length in liquid crystals will be only a few tens of microns in the frequency range of our measurements. This implies that the surface effects in the nematic and smectic A phases may play a dominant role in the measured thermal effusivity values in these phases, as the surface layers in liquid crystals always show complex molecular alignment. The closeness in the thermal effusivity values of 8OCB in the smectic A and nematic phases is, however, a very reasonable observation as the thermal conductivity and specific heat capacity in these two phases are almost constant.

Also, a comparison of the two materials shows that the thermal effusivities in the nematic and isotropic phases of 7OCB are slightly less than those of 8OCB in the corresponding phases. This can be explained using the simple arguments introduced by Rondelez et al., in which they assume that the thermal conductivity is strongly affected by the shape of the liquid crystal molecule [16]. Considering the molecules

Fig. 6. Logarithmic plot connecting the square root of modulation frequency and the normalized PA signal amplitudes for 8OCB. The *straight lines* correspond to a linear fit to the experimental data

Table 1. The thermal effusivity values in various mesophases of 8OCB and 7OCB

Liquid Crystal	Thermal effusivity e_s in W s$^{1/2}$ cm^{-2} K^{-1}		
	Smectic A	Nematic	Isotropic
8OCB	0.056 ± 0.003	0.057 ± 0.003	0.071 ± 0.003
7OCB	No smectic phase	0.051 ± 0.003	0.068 ± 0.003

Fig. 7. Logarithmic plot connecting the square root of modulation frequency and the normalized PA signal amplitudes for 7OCB. The *straight lines* correspond to a linear fit to the experimental data

as rigid rods and assuming that the intramolecular thermal conductivity is exceedingly high with respect to that of the intermolecular, it follows that 7OCB, a shorter homologue of 8OCB, should possess a lower thermal conductivity and hence a lower thermal effusivity than 8OCB.

4 Conclusions

In conclusion, we have successfully used an open photo-acoustic cell configuration for the thermal characterisation of transparent liquids and liquid crystals. The thermal effusivi-ties in the various mesophases of two stable liquid crystals, 8OCB and 7OCB, have been evaluated using the open cell photoacoustic configuration. The possibility of the influence of surface effects of the liquid crystals on the thermal effusiv-ity values is highlighted. The present experimental method is quite simple and less time consuming than earlier methods, and a combination of the present method with the earlier reported photoacoustic configurations can be used for a com-plete thermal characterisation of liquid crystals.

References

1. F. Mercuri, U. Zammit, M. Marinelli: Phys. Rev. E **57**, 596 (1998)
2. R.J. Birgeneav, C.W. Garland, G.B. Kasting, B.M. Ocko: Phys. Rev. A **24**, 2624 (1981)
3. G.B. Kasting, K.J. Lushington, C.W. Garland: Phys. Rev. B **22**, 321 (1980)
4. J.D. LeGrange, J.M. Mochel: Phys. Rev. A **23**, 3215 (1981)
5. C.W. Garland, G.B. Kasting, K.J. Lushington: Phys. Rev. Lett **43**, 1420 (1979)
6. U. Zammit, M. Marinelli, R. Pizzoferrato, F. Scudieri, S. Martellucci: Phys. Rev. A **41**, 1153 (1990)
7. G. Puccetti, R.M. Leblanc: J. Chem. Phys. **108**, 7258 (1998)
8. M. Marinelli, F. Mercuri, U. Zammit, F. Scudieri: Phys. Rev. E **58**, 5860 (1998)
9. L.F. Perondi, L.C.M. Miranda: J. Appl. Phys. **62**, 2955 (1987)
10. N.A. George, C.P.G. Vallabhan, V.P.N. Nampoori, A.K. George, P. Rad-hakrishnan: J. Phys.: Condens. Matter **13**, 365 (2001)
11. A. Rosencwaig, A. Gersho: J. Appl. Phys **47**, 64 (1976)
12. *CRC Handbook of Chemistry: Physics*, Sects. 5 and 6 (CRC Press, Boca Raton 1999)
13. V.K. Agarwal, K.M. Khamis, V.P. Arora: Indian J. Pure Appl. Phys. **26**, 614 (1988)
14. P.E. Cladis, R.K. Bogardur, D. Aadsen: Phys. Rev. A **18**, 2292 (1978)
15. P.G. deGennes: *The Physics of Liquid Crystals*, Chapt. 2 (Clarendon, Oxford 1974)
16. F. Rondelez, W. Urbach, H. Hervet: Phys. Rev. Lett. **41**, 1058 (1978)